A THREE-DIMENSIONAL NUMERICAL MODEL FOR LARGE-SCALE RIVER FLOW WITH A NEW MODE-SPLITTING TECHNIQUE

Yasuo NIHEI[(1)], Yuichi KATO[(2)] and Keita SATO[(3)]

[(1)]Department of Civil Engineering, Tokyo University of Science, 2641 Yamazaki, Noda-shi, Chiba, 278-8510, Japan, phone: +81-4-7124-1501; fax: +81-4-7123-9766; e-mail: nihei@rs.noda.tus.ac.jp

[(2)] Asia Air Survey Co. Ltd., 1-2-2 Manpukuji, Aso-ku, Kawasaki-shi, Kanagawa, 215-0004, Japan, phone: +81-44-969-7310; fax: +81-44-965-0037; e-mail: yui.katou@ajiko.co.jp

[(3)]Docon Co. Ltd., 1-5-4-1 Atsubetsu-chuo, Atsubetsu-ku, Sapporo, 004-8585, Japan, phone: +81-11-801-1587; fax: +81-11-801-1588; e-mail: ks1495@docon.jp

ABSTRACT

A three-dimensional (3D) numerical method for large-scale river flow with a new mode-splitting technique and parallel computation is developed. To remove the severe limitation of the computational time interval required for the 3D calculation in previous mode-splitting techniques, we present a new mode-splitting technique with high numerical stability and reduced computational time. The present model is applied to a flood flow computation of the Edo River, Japan. Good agreement is obtained between the model simulation and field measurements. More importantly, the computational time of the present model is only 0.4% of that of a normal 3D model without the mode-splitting and parallel processing techniques.

Keywords: river flow; three-dimensional numerical method; mode-splitting technique; flood flow

1 INTRODUCTION

A modern CFD (Computational Fluid Dynamics) technique is one of the promising tools for river management and flood control due to the recent progress of computational resources (*e.g.*, Bates et al., 2005). For environmental problems of a river system over the whole river basin, it is necessary to develop an accurate river-flow model that reduces the computational load inherent for numerical simulations of large-scale, complicated river-flow fields.

Most river-flow computations have been done using one- or two-dimensional numerical models. However, flow structures in rivers are generally very complex due to

irregular topography such as meandering channels, and hence three-dimensional (3D) models should be adopted for river-flow simulations. Although 3D computations of river flows have been done (*e.g.*, Biron et al., 2004; Zanichelli et al., 2004), the computational domains of 3D numerical simulations have been limited to local areas of a river due to the heavy computational load. Therefore, 3D computations for a large-scale river flow have not been performed in previous works for river-flow simulations.

In the present study, we develop a new 3D river-flow model that can be applied to a large-scale river flow with a reduced computational load. For this purpose, we incorporate a new mode-splitting technique and parallel processing. In general, the mode-splitting technique separates the calculation of the vertically averaged two-dimensional (2D) equation for fluid motion from the computation of the 3D governing equation (Madala and Piacsek, 1977), and then one can adopt a time interval for the 3D computation larger than that for the 2D computation. Mode splitting has been widely used in 3D ocean current models, such as POM (Princeton Ocean Model; Blumberg and Mellor, 1983). For further computational efficiency, we present a new mode-splitting technique in which the Courant, Friedrichs and Levy (CFL) stability condition may not limit the computational time interval in the 3D computation. We apply the present 3D river-flow model with the new mode-splitting technique to the flood flow computation of the Edo River in Japan and compare the measured results obtained by the authors (Sato et al., 2004) to validate the numerical performance of the present model.

2 OUTLINE OF PRESENT 3D RIVER-FLOW MODEL

2.1 FUNDAMENTAL CONCEPT OF THE NEW MODE-SPLITTING TECHNIQUE

In the previous mode-splitting procedure, 2D and 3D calculations are separately performed. As shown in Fig. 1(a), the time interval of the 2D calculation (external mode) Δt_e is smaller than that of the 3D calculation (internal mode) Δt_i. This is attributed to the differences of velocities adopted in the CFL conditions, which correspond to the gravity-wave speed and current velocity in 2D and 3D calculations, respectively. In applying the mode splitting to river-flow simulations, however, the difference of the time intervals between the 2D and 3D calculations is much smaller than that in coastal current simulations because the water depth in rivers is generally shallower than that in coastal regions. Furthermore, in the previous mode splitting, the setting of time interval Δt_i in the 3D calculation is limited to the CFL conditions.

To avoid these problems in the present mode-splitting technique, the CFL stability condition may not limit the computational time interval in the 3D computation;

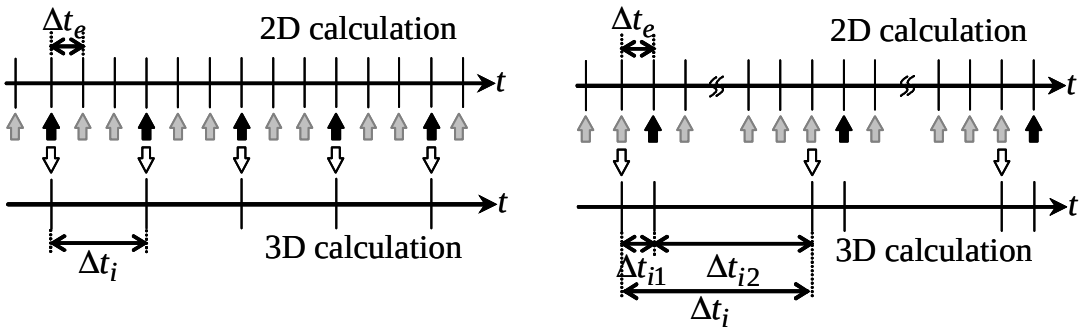

(a) Previous technique (b) Present technique

Fig. 1 Comparison of numerical procedures in previous and present mode-splitting techniques.

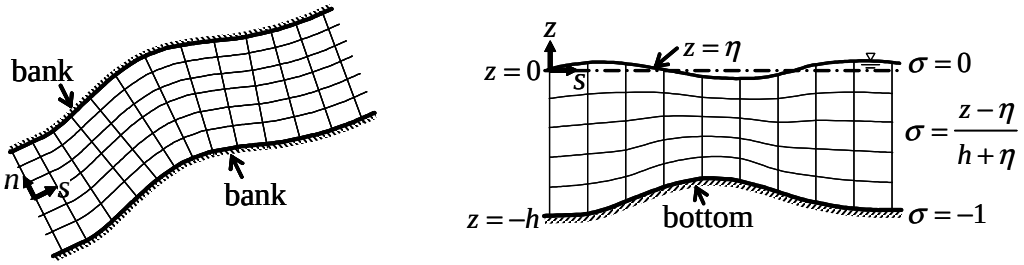

(a) Horizontal coordinate (b) Vertical coordinate

Fig. 2 Coordinates adopted in the present model.

therefore, the present technique can reduce the computational load of the 3D calculation. In the present technique, as depicted in Fig. 1(b), the time interval Δt_i in the 3D calculation is separated into two parts, Δt_{i1} and Δt_{i2}. During Δt_{i1}, the 2D and 3D calculations are done as in the previous mode-splitting technique. On the other hand, during Δt_{i2}, only the 2D calculation is performed due to the assumption that temporal variations of the vertical velocity profile may be small compared to that of the depth-averaged velocity. Since the 3D calculation is not carried out during Δt_{i2}, the setting of Δt_{i2} is not influenced by the CFL condition for the 3D calculation. Therefore, the present mode-splitting technique can appreciably reduce the computational load.

2.2 COORDINATES AND GOVERNING EQUATIONS

The present 3D river-flow model is based on the hydrostatic assumption and uses orthogonal curvilinear and sigma coordinates (s,n,σ) for the horizontal and vertical directions, respectively, as shown in Fig. 2 (Philips, 1957). To reduce the computational load in the 3D river-flow computation, the new mode splitting and parallel processing are incorporated into the 3D river-flow model. The continuity and momentum equations for the 3D numerical computation are given as follows:

$$\frac{1}{1+N}\frac{\partial}{\partial s}\left(Du_s\right)+\frac{\partial}{\partial n}\left(Du_n\right)+\frac{Du_n}{\left(1+N\right)R}+\frac{\partial w^*}{\partial\sigma}+\frac{\partial D}{\partial t}=0\,, \tag{1}$$

$$\begin{aligned}&\frac{\partial u_s}{\partial t}+\frac{u_s}{1+N}\frac{\partial u_s}{\partial s}+u_n\frac{\partial u_s}{\partial n}+\frac{w^*}{D}\frac{\partial u_s}{\partial\sigma}+\frac{u_s u_n}{\left(1+N\right)R}\\&=-\frac{g}{1+N}\frac{\partial\left(D+z_b\right)}{\partial s}+\frac{1}{1+N}\frac{\partial}{\partial s}\left(\frac{2A_H}{1+N}\frac{\partial u_s}{\partial s}\right)+\frac{\partial}{\partial n}\left\{A_H\left(\frac{\partial u_s}{\partial n}+\frac{1}{1+N}\frac{\partial u_n}{\partial s}\right)\right\},\\&\quad+\frac{1}{D}\frac{\partial}{\partial\sigma}\left(\frac{A_V}{D}\frac{\partial u_s}{\partial\sigma}\right)-\frac{aC_b}{2}u_s\sqrt{{u_s}^2+{u_n}^2}\end{aligned} \tag{2}$$

$$\begin{aligned}&\frac{\partial u_n}{\partial t}+\frac{u_s}{1+N}\frac{\partial u_n}{\partial s}+u_n\frac{\partial u_n}{\partial n}+\frac{w^*}{D}\frac{\partial u_n}{\partial\sigma}-\frac{{u_s}^2}{\left(1+N\right)R}\\&=-g\frac{\partial\left(D+z_b\right)}{\partial n}+\frac{1}{1+N}\frac{\partial}{\partial s}\left\{A_H\left(\frac{\partial u_s}{\partial n}+\frac{1}{1+N}\frac{\partial u_n}{\partial s}\right)\right\}\\&\quad+\frac{\partial}{\partial n}\left(2A_H\frac{\partial u_n}{\partial n}\right)+\frac{1}{D}\frac{\partial}{\partial\sigma}\left(\frac{A_V}{D}\frac{\partial u_n}{\partial\sigma}\right)-\frac{aC_b}{2}u_n\sqrt{{u_s}^2+{u_n}^2}\end{aligned}\,, \tag{3}$$

where u_s, u_n and w^* are the velocities in the *s*, *n* and σ directions, *g* is the gravitational acceleration, *D* is total water depth, z_b is the level of the river bed, R is the radius of curvature of the main channel, $N=n/R$, A_H and A_V represent the horizontal and vertical eddy viscosities, respectively, and *a* and C_b are the density and drag coefficients of vegetation, respectively. In the present study, A_H and A_V are modeled by a primitive zero-equation turbulence model.

The governing equations for the 2D calculation are depth-averaged continuity and momentum equations, expressed as

$$\frac{\partial\eta}{\partial t}+\frac{1}{1+N}\frac{\partial}{\partial s}\left(DU_s\right)+\frac{\partial}{\partial n}\left(DU_n\right)+\frac{DU_n}{\left(1+N\right)R}=0\,, \tag{4}$$

$$\begin{aligned}&\frac{\partial U_s}{\partial t}+\frac{U_s}{1+N}\frac{\partial U_s}{\partial s}+U_n\frac{\partial U_s}{\partial n}+\frac{U_s U_n}{\left(1+N\right)R}\\&=-\frac{g}{1+N}\frac{\partial\left(D+z_b\right)}{\partial s}+\frac{1}{1+N}\frac{\partial}{\partial s}\left(\frac{2A_{H2D}}{1+N}\frac{\partial U_s}{\partial s}\right)\\&\quad+\frac{\partial}{\partial n}\left\{A_{H2D}\left(\frac{\partial U_s}{\partial n}+\frac{1}{1+N}\frac{\partial U_n}{\partial s}\right)\right\}-\left(\frac{C_{fb}}{D}+\frac{aC_b}{2}\right)U_s\sqrt{{U_s}^2+{U_n}^2}-G_s\end{aligned}\,, \tag{5}$$

$$\frac{\partial U_n}{\partial t}+\frac{U_s}{1+N}\frac{\partial U_n}{\partial s}+U_n\frac{\partial U_n}{\partial n}-\frac{{U_s}^2}{(1+N)R}$$
$$=-g\frac{\partial(D+z_b)}{\partial n}+\frac{1}{1+N}\frac{\partial}{\partial s}\left\{A_{H2D}\left(\frac{\partial U_s}{\partial n}+\frac{1}{1+N}\frac{\partial U_n}{\partial s}\right)\right\} \quad , \qquad (6)$$
$$+\frac{\partial}{\partial n}\left(2A_{H2D}\frac{\partial U_n}{\partial n}\right)-\left(\frac{C_{fb}}{D}+\frac{aC_b}{2}\right)U_n\sqrt{{U_s}^2+{U_n}^2}-G_n$$

where U_s and U_n are the depth-averaged velocities in the s and n directions, respectively, η is the water elevation, A_{H2D} represents the depth-averaged horizontal eddy viscosity and C_{fb} denotes the coefficient of the bottom friction ($=gn^2/D^{1/3}$, n: Manning's roughness coefficient). G_s and G_n on the right side of Eqs. 5 and 6 express the correction terms, which are introduced to incorporate the 3D computational results into the 2D calculation.

2.3 NUMERICAL PROCEDURE

The numerical procedure of the present 3D river flow model with the new mode-splitting technique is divided into two parts, which correspond to the period of Δt_{i1} (step 1) and that of Δt_{i2} (step 2). In step 1, the 2D and 3D calculations are carried out using Eqs. 1-6; only the 2D calculation is performed in step 2. The parallel processing technique is also introduced into the code of the model used here. The other details of the numerical procedure are omitted in this paper.

3 APPLICATION OF THE PRESENT 3D MODEL TO FLOOD FLOW COMPUTATION

3.1 COMPUTATIONAL CONDITIONS

To examine the fundamental performance of the present river-flow model, we apply the present model to a large-scale river-flow

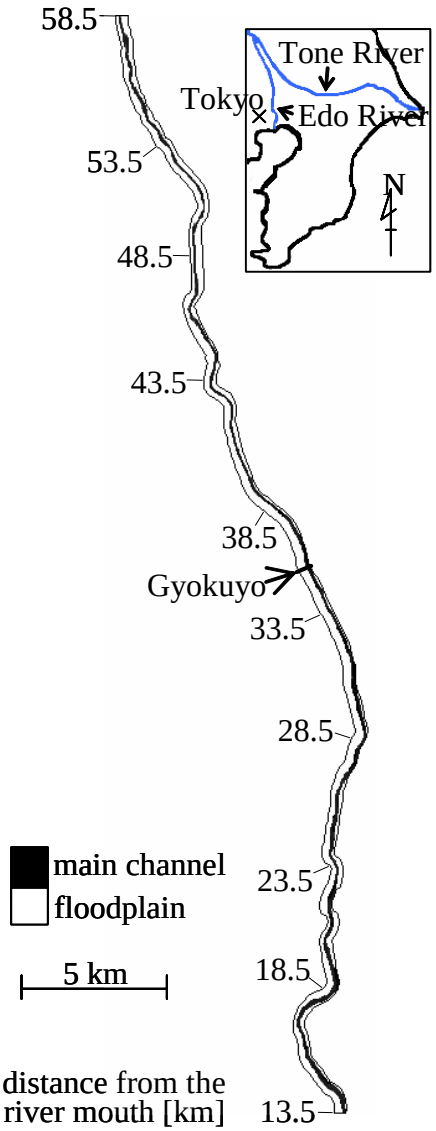

Fig. 3 Computational domain.

Table 1 Computational conditions.

Domain size	45000 m×670 m
Grid number	225×67×10
n	0.031 $m^{-1/3}s$ (21.1 km～58.5 km) 0.024 $m^{-1/3}s$(13.5 km～21.1 km)
C_b	2.00
a	1.18 m^{-1}
$\Delta t_e\ (=\ \Delta t_{i1})$	0.50 s

Table 2 Conditions of the ratio of the time interval $\Delta t_i/\Delta t_e$ and the number of CPUs N_c.

	$\Delta t_i/\Delta t_e$	N_c
Case1	1	1
Case2	1	10
Case3	100	1
Case4	100	10

computation. The site for the computation is the Edo River, which flows near Tokyo, Japan, as shown in Fig. 3. The average width of compound cross sections of the Edo River is about 400 m.

The total length of the computational domain is 45 km. The upper and lower sections of the computational domain of the Edo River are located at 58.5 km and 13.5 km upstream from the river mouth. The computational period is from Aug. 9 to Aug. 12, 2003, when a hydrologic event occurred due to the attack of typhoon No. 0310. As the boundary conditions at the upper and lower boundaries, we set the measured values for the water elevations and an open boundary condition for the velocities. At the lateral boundary, we apply a no-slip condition. At the water surface and bottom boundaries, we employ slip and wall conditions, respectively. As the initial condition, the velocities are set to zero and the water elevation is given as the interpolated measured data.

Table 1 summarizes the parameters used in the computation. The grid numbers are 225, 67 and 10 in the *s*, *n* and σ directions, respectively. To match the computed and measured water elevations, we set two values of Manning's roughness coefficient *n* for the upper and lower reaches. The computational time intervals of Δt_e and Δt_{i1} are

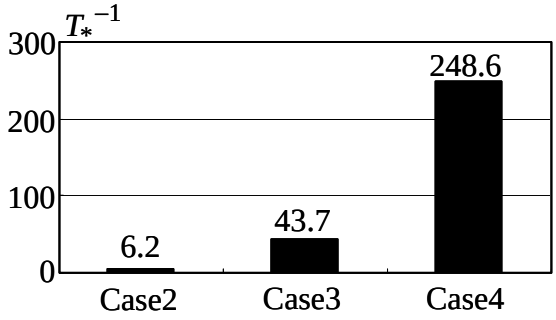

Fig. 4 Reciprocal of the normalized CPU time T_* in each case.

set at 0.50 s. To check the computational efficiency of the present model, we set up four cases for the time interval Δt_i and number of CPUs N_c, as indicated in Table 2.

3.2 CPU TIME

To compare the CPU time in each case, Fig. 4 represents the reciprocal of the normalized CPU time T_* which is the ratio of the CPU time in each case to that of case1. The reciprocals of T_* are 6.2 and 43.7 in case2 and case3, respectively. In case4, in which the present mode-splitting technique and parallel processing are used, the reciprocal of T_* is 248.6. It should be noted that the computational time of the present 3D river-flow model with the new mode-splitting technique and parallel processing amounts to only 0.4% of that of the normal 3D model without these techniques. This fact demonstrates that the present model can appreciably reduce the computational time by introducing the new mode-splitting technique and parallel processing.

3.3 COMPARISON OF MEASURED AND COMPUTED RESULTS

To examine the fundamental validity of the present model, we compare the computed results with the measured data. Figure 5 displays the temporal variations of the water elevation and discharge at Gyokuyou, which is located 35.5 km upstream from the river mouth. In the figure, the computed and measured results are shown. The computed water elevation is in good agreement with the measured water elevation. From the results of the discharge, the difference between the computed and measured discharges is almost less than 10% of the discharge, indicating that the computed discharge is also in good agreement with the measured discharge. It is worth noting from these results that the present model can simulate accurately the temporal variations of the water elevation and discharge.

The contours of the computed and measured streamwise velocities in the cross section at Gyokuyou are shown in Fig. 6. The result at a rising stage (18:00 on Aug. 9)

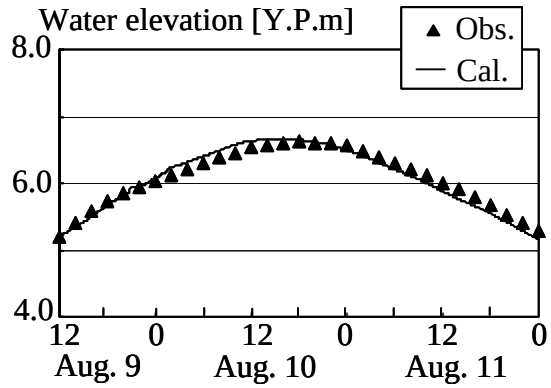

(a) Water elevation

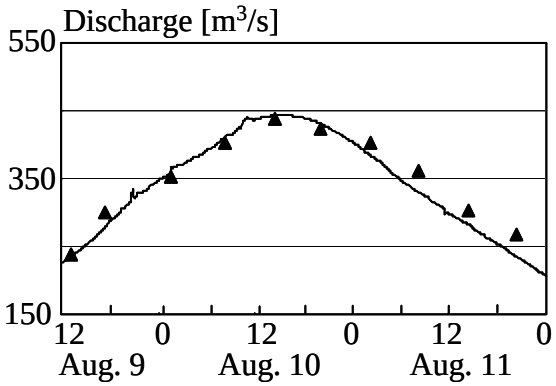

(b)Discharge

Fig. 5 Comparison of the measured and computed results at Gyokuyou.

is drawn in the figure. Figure 6 indicates that the overall pattern for the computed velocity contour gives acceptable agreement with that of the measured data except for the velocity near both banks. The discrepancy is caused by the treatment of the fluid drag due to the vegetation located near the banks. The model for the vegetation drag should be improved in future work.

The above comparison of the computed and measured results indicates that the computed results give good agreement with the measured results, demonstrating the fundamental validity of the present 3D model for flood flow computations.

4 CONCLUSIONS

The main conclusions of the present study are as follows:

1) A three-dimensional numerical method for large-scale river flow with a new mode-splitting technique and parallel processing is developed. To remove the severe limitation of the computational time interval for the 3D calculation in previous

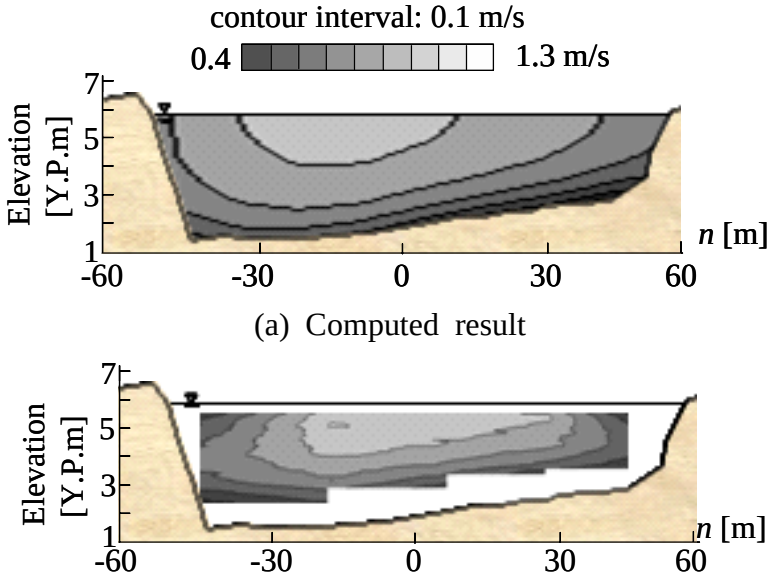

(a) Computed result

(b) Measured result

Fig. 6 Contours of the streamwise velocity in the main channel at Gyokuyou at a rising stage (18:00 on Aug. 9, 2003).

mode-splitting techniques, we present a new mode-splitting technique with high numerical stability and a reduced computational load.

2) The present model is applied to the flood flow computation of the Edo River in Japan. Good agreement is obtained between the model simulation and field measurements. These results suggest high performance of the present model for flood flow computations.
3) More importantly, the computational time of the present model with the new mode-splitting technique and parallel processing amounts to only 0.4% of that of the normal 3D model without these techniques.

ACKNOWLEDGEMENTS

This study was partially supported by the Japan Society for the Promotion of Science, Grant-in-Aid for Scientific Research (C) (2) (No. 16560453). The authors would like to express their deep thanks to Dr. Yamasaki and Mr. Machida for their help in performing some of the numerical simulations in the present study.

REFERENCES

Bates, P. D., Lane, S. N. and Ferguson, R. I. (2005), Computational fluid dynamics, *John Wiley & Sons*, 1-531.

Biron, P. M., Ramamurthy, A. S. and Han, S. (2004), Three-dimensional numerical modeling of mixing at river confluences, *J. Hydraul. Eng., ASCE*, 130(3), 243-253.

Blumberg, A. F. and Mellor, G. L. (1983), Diagnostic and prognostic numerical circulation studies of the South Atlantic Bight, *J. Geophys. Res.*, 88(C8), 4579-4592.

Madala, R. V. and Piacsek, S. A. (1977), A semi-implicit numerical model for baroclinic oceans, *J. Comp. Phys.*, 23, 167-178.

Phillips, N. A. (1957), A coordinate system having some special advantages for numerical forecasting, *J. Meteor.*, 14, 184-185.

Sato, K., Nihei, Y., Kimizu, A. and Iida, Y. (2004), An application of high-resolution acoustic Doppler current profiler into a flood-flow measurement, *Annual J. Hydraul. Eng., JSCE*, 48, 763-768 (in Japanese).

Zanichelli, G., Caroni, E. and Fiorotto, V. (2004), River bifurcation analysis by physical and numerical modeling, *J. Hydraul. Eng., ASCE*, 130(3), 237-242.